

(NASA-TM-78210) CONTINUOUS-FLOW
ELECTROPHORESIS: MEMBRANE-ASSOCIATED
DEVIATIONS OF BUFFER pH AND CONDUCTIVITY
(NASA) 23 p HC A02/MF A01

CSSL 07D

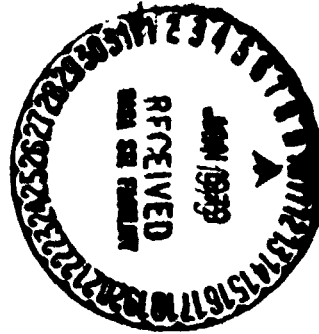
N79-13101

Unclas

63/25 40370

NASA TECHNICAL MEMORANDUM

NASA TM-78210



CONTINUOUS-FLOW ELECTROPHORESIS: MEMBRANE-ASSOCIATED
DEVIATIONS OF BUFFER pH AND CONDUCTIVITY

By Adam J. K. Smolka and Janice K. McGuire
Space Sciences Laboratory

November 1978

NASA

*George C. Marshall Space Flight Center
Marshall Space Flight Center, Alabama*

TECHNICAL REPORT STANDARD TITLE PAGE

1. REPORT NO. NASA TM-78210	2. GOVERNMENT ACCESSION NO.	3. RECIPIENT'S CATALOG NO.	
4. TITLE AND SUBTITLE Continuous-Flow Electrophoresis: Membrane-Associated Deviations of Buffer pH and Conductivity		5. REPORT DATE November 1978	
		6. PERFORMING ORGANIZATION CODE	
7. AUTHOR(S) Adam J. K. Smolka* and Janice K. McGuire**		8. PERFORMING ORGANIZATION REPORT #	
9. PERFORMING ORGANIZATION NAME AND ADDRESS George C. Marshall Space Flight Center Marshall Space Flight Center, Alabama 35812		10. WORK UNIT NO.	
		11. CONTRACT OR GRANT NO.	
		13. TYPE OF REPORT & PERIOD COVERED Technical Memorandum	
12. SPONSORING AGENCY NAME AND ADDRESS National Aeronautics and Space Administration Washington, D.C. 20546		14. SPONSORING AGENCY CODE	
15. SUPPLEMENTARY NOTES Prepared by Space Sciences Laboratory, Science and Engineering *Visiting Scientist, Universities Space Research Association **Department of Microbiology, Athens State College, Athens, Alabama			
16. ABSTRACT <p>The deviations in buffer pH and conductivity which occur near the electrode membranes in continuous-flow electrophoresis were studied in the Beckman charged particle electrophoresis system and the Hannig FF-5 preparative electrophoresis instrument. The nature of the membranes separating the electrode compartments from the electrophoresis chamber, the electric field strength, and the flow rate of electrophoresis buffer were all found to influence the formation of the pH and conductivity gradients. Variations in electrode buffer flow rate and the time of electrophoresis were less important. The results obtained supported the hypothesis that a combination of Donnan membrane effects and the differing ionic mobilities in the electrophoresis buffer was responsible for the formation of the gradients. The significance of the results for the design and stable operation of continuous-flow electrophoresis apparatus is discussed.</p>			
17. KEY WORDS		18. DISTRIBUTION STATEMENT <i>Annelle K. Single</i> Unclassified - Unlimited	
19. SECURITY CLASSIF. (of this report) Unclassified	20. SECURITY CLASSIF. (of this page) Unclassified	21. NO. OF PAGES 22	22. PRICE NTIS

ACKNOWLEDGMENTS

The authors wish to thank the Universities Space Research Association for financial support which made this work possible. We thank also Dr. Robert Snyder of the Space Sciences Laboratory at the Marshall Space Flight Center and Dr. George Sachs of the Membrane Biology Laboratory at the University of Alabama (Birmingham) Medical School for helpful discussions and provision of laboratory facilities during the preparation of this manuscript.

TABLE OF CONTENTS

	Page
I. INTRODUCTION	1
II. APPARATUS	3
A. Beckman Continuous-Flow Electrophoresis System	3
B. Hannig FF-5 Free-Flow Electrophoresis Separator	4
C. Continuous-Flow Electrophoresis Buffer	5
III. METHODS	6
IV. RESULTS	6
V. DISCUSSION	11
REFERENCES	16

PRECEDING PAGE BLANK NOT FILMED

LIST OF ILLUSTRATIONS

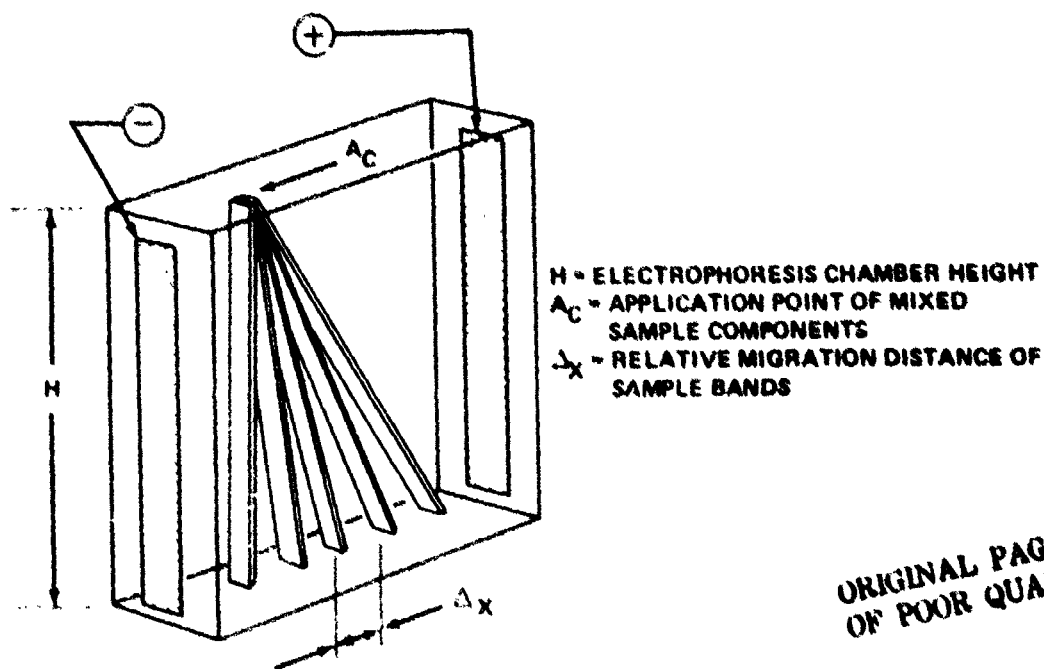
Figure	Title	Page
1.	Principle of continuous-flow electrophoresis	1
2.	Schematic diagram of Beckman CPE	4
3.	pH and conductivity profiles of R-1 buffer collected from the Beckman CPE under a variety of conditions	7
4.	Effect of time on the change in pH in Region A and on the migration distance of the pH discontinuity	9
5.	Effect of electrode buffer flow rate on the change in pH in Region A and on the migration distance of the pH discontinuity	9
6.	Effect of curtain flow rate on the change in pH in Region A and on the migration distance of the pH discontinuity	10
7.	Effect of electric field strength on the change in pH in Region A and on the migration distance of the pH discontinuity	10
8.	Conductivity and pH profile of R-1 buffer collected from Beckman CPE, with dilute R-1 buffer in both electrode compartments	11
9.	Conductivity and pH profile of R-1 buffer collected from Hannig FF-3 electrophoresis apparatus	12

TECHNICAL MEMORANDUM

CONTINUOUS-FLOW ELECTROPHORESIS: MEMBRANE-ASSOCIATED
DEVIATIONS OF BUFFER pH AND CONDUCTIVITY

I. INTRODUCTION

First described by Svensson and Brattsten [1], continuous-flow electrophoresis is characterized by a film of buffer moving through a direct current electric field placed normal to the direction of flow. The sample mixture is injected into the buffer curtain as a narrow streak, and separation of the charged sample ions occurs as a function of their surface charge density, the electrical field strength, and buffer curtain flow rate. The separated zones are collected by an array of tubes which fractionate the buffer curtain after its passage through the field. The principle is illustrated in Figure 1. Originally designed for use with support media such as filter paper and glass powders, continuous-flow electrophoresis has more recently been adapted for free-flowing buffer systems by Barrolier et al. [2] and most notably by Hannig [3].



ORIGINAL PAGE IS
OF POOR QUALITY

Figure 1. Principle of continuous-flow electrophoresis.

Effective removal of the Joule heat generated by the passage of electrical current is of primary importance in electrophoresis. In continuous-flow electrophoresis, the buffer curtain is confined to a thin film between thermostatted surfaces approximately 1-mm apart; the resulting high surface-to-volume ratio provides very efficient cooling.

Attempts to eliminate or minimize electrophoretic thermal convection arising from Joule heat have focused on the use of solid support media such as starch or polyacrylamide gels, density gradients, Sephadex, or glass beads. While these stratagems are successful and widely used on the analytical scale, they are all difficult to scale up and are largely unsuited for cell separation. In continuous-flow electrophoresis, anticonvective stabilization is accomplished without the use of solid support media. The separation buffer flows through the narrow space between the electrodes at a velocity sufficient to overcome the effects of gravitation and convection, especially in the bulk of the medium remote from the walls. The use of a free-flowing buffer allows separation of living cells which are too large to migrate through the pore structure of anti-convective gels, while the rapid flow of buffer minimizes sedimentation effects. In addition, continuous-flow electrophoresis allows uninterrupted withdrawal of separated zones as long as the sample mixture is injected into the buffer curtain. The amount of material to be processed is limited only by the long-term stability of the apparatus itself and the time available.

The disadvantages of continuous-flow electrophoresis are related to sample streak stability and the effectiveness of gravitational stabilization at low curtain flow rates, which are desirable for optimum resolution. Strickler and Sacks [4] have defined two phenomena which lead to sample band broadening and distortion. First, the parabolic flow velocity profile of the buffer curtain results in sample ions near the walls having a longer residence time in the field and, consequently, experiencing a greater lateral displacement than ions near the center of the chamber. Secondly, sample ions near the walls are entrained in the electro-osmotic flow of buffer towards the cathode. The net results of these perturbations is distortion of the sample streak into a crescent shape, with attendant loss of resolution.

More recent studies [5, 6, 7] have considered the specific effects of transverse and longitudinal temperature gradients on the overall stability of the buffer curtain in an effort to determine whether continuous-flow electrophoresis in zero-gravity would show benefits over terrestrial electrophoresis. The present study suggests the existence of a hitherto overlooked convective instability which is laterally oriented in the buffer curtain. This instability is generated as a result of changes in buffer pH and conductivity near the electrode

membranes which distort the otherwise uniform electric field, thereby giving rise to temperature gradients across the width of the chamber. The data presented in this report seek to describe the preceding pH and conductivity gradients and their relationship to electric field strength. In addition, a mechanism for the formation of the gradients is proposed.

II. APPARATUS

A. Beckman Continuous-Flow Electrophoresis System

Figure 2 shows a schematic diagram of the Beckman charged particle electrophoresis (CPE) instrument. The electrophoresis chamber is defined by a pair of Lucite plates separated by a Teflon spacer and sealed with an O-ring. The chamber dimensions are 1.5-mm thickness, 44-mm width, and 50-cm length. Platinum wire electrodes 30-cm long are housed in vertical recesses machined into both sides of the back plate. In this study, cellulose acetate dialysis membranes (Spectrapor 2, which is 25- μ m thick, has a molecular weight cutoff of 12 000-14 000, and is sealed in place with O-rings) separated the electrode recesses from the electrophoresis chamber. Both recesses are equipped with platinum electrodes which sense electric field strength across the curtain. An electrode buffer pump circulates cold (4°C) concentrated electrophoresis buffer through the electrode recesses to remove electrode decomposition products and Joule heat. A peristaltic pump circulates curtain buffer through heat exchange coils, immersed in a water-ethylene glycol bath at 4°C, to a pressure equalization bottle and thence through a 0.45- μ m millipore filter and flow rate meter into the electrophoresis chamber. Curtain buffer leaves the chamber via 48 ports 1-mm apart located across the bottom of the electrophoresis space. The ports discharge their fraction of the buffer curtain into an array of test tubes. The front Lucite plate incorporates a milled recess through which water at 4°C is circulated, thus removing Joule heat from the flowing curtain buffer. A window located 5-cm above the collection port is illuminated from behind by a straight-line incandescent filament equipped with a lens and horizontal slit which images the light source in the plane of the buffer curtain. This optical device allows visual examination of the cross-sectional profile of sample streaks. A controlled-rate syringe pump (Sage Instruments, Inc., Model 355) injects the sample through a stainless steel needle located above the electrode space in the central upper third of the chamber.

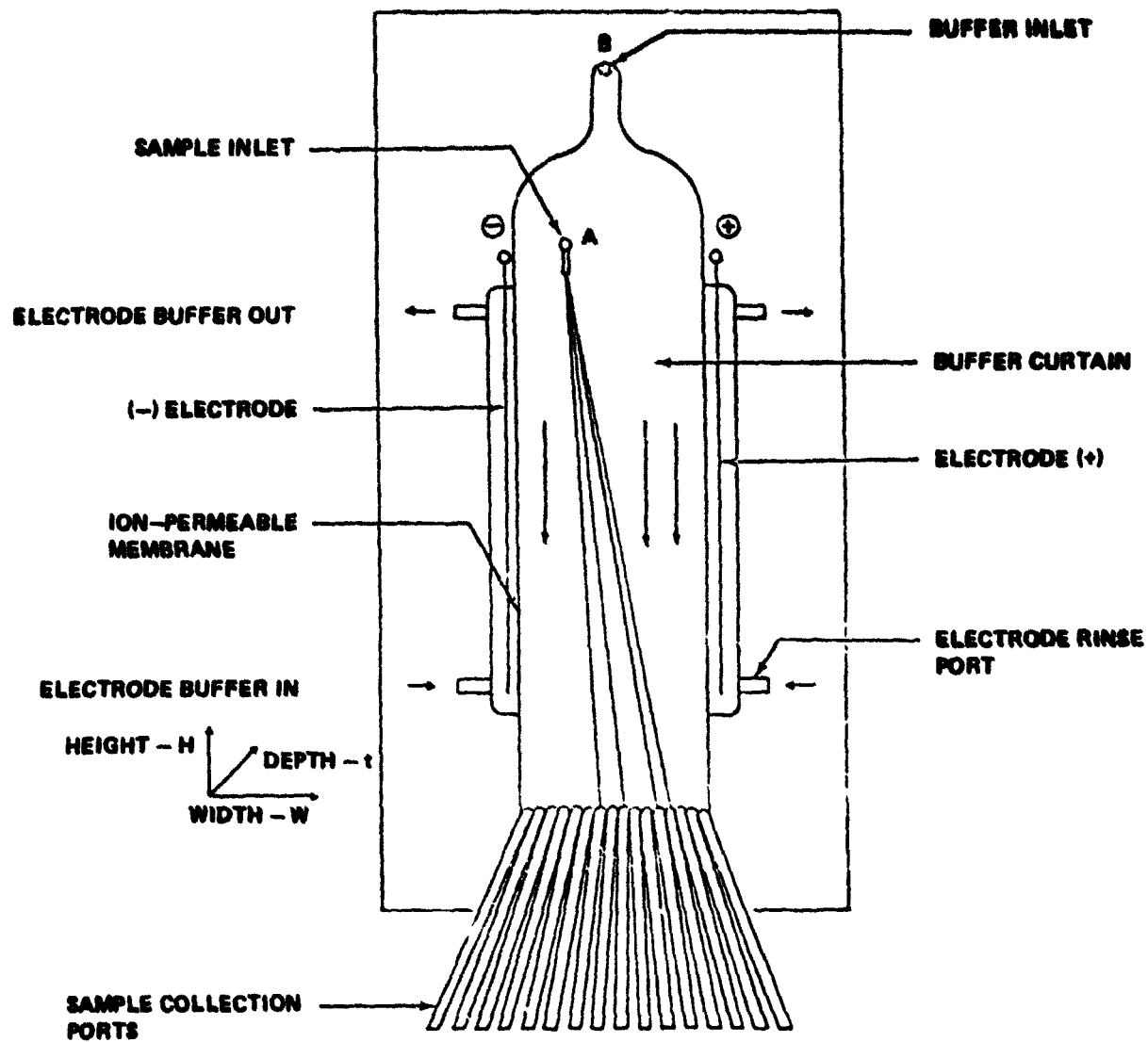


Figure 2. Schematic diagram of Beckman CPE.

B. Hannig FF-5 Free-Flow Electrophoresis Separator

This instrument differs only in detail from the Beckman CPE previously described and is adequately discussed in the literature [8]. The FF-5 was used in this study because its electrode compartments are designed to take ion-exchange membranes rather than the dialysis membranes fitted on the CPE. In accordance with the procedures of Hannig [8], the anode compartment was fitted with a cation exchange membrane, while the cathode was fitted with an anion exchange membrane (Ionics Inc., Watertown, Massachusetts).

C. Continuous-Flow Electrophoresis Buffer

A well-characterized phosphate buffer, formulated by Seaman [9] for a proposed zero-gravity continuous-flow electrophoresis separation of polystyrene latex particles [10], was used in this study. During terrestrial evaluation of the proposed Space Processing Applications Rocket experiment, this buffer was found to undergo pH and conductivity changes similar to those reported by Brattsten [11] with veronal and acetate buffers, by Zeiller et al. [12] who used triethanolamine/glycine and HEPES/glycine media, and by Strickler [13] using Beckman B-2 veronal buffer at pH 8.6.

The composition of R-1 buffer is given in Table 1, and its properties were as follows:

Conductivity at 25°C — 3.49×10^{-3} mho/cm

pH at 23°C — 7.21

Viscosity at 25°C — 0.898 cp

Osmolality — 56.5 milliosmoles/kg.

All reagents used in making up the R-1 buffer were of analytical reagent grade, with assays of 99-percent purity by weight. Distilled water was obtained by a two-stage distillation in Pyrex ware and had a conductivity of 1.75×10^{-6} mho/cm at 25°C.

TABLE 1. COMPOSITION OF R-1 BUFFER

Substance	Molecular Weight	10X	1X	
		(gm/liter)	(gm/liter)	(Millimolarity)
Na ₂ HPO ₄ ·7H ₂ O	268.07	4.72	0.472	1.76
KH ₂ PO ₄	136.09	0.50	0.05	0.367
Na ₂ EDTA·2H ₂ O	372.24	1.251	0.125	0.336

III. METHODS

The continuous-flow electrophoresis apparatus was filled with R-1 curtain buffer and 10X concentrated R-1 electrode buffer. The flow rates of both buffers were adjusted to required values using variable flow meters. Curtain fractions were collected after 10 min for baseline measurements of buffer pH and conductivity. Following establishment of the electric field, and its adjustment to required values of voltage and current, the apparatus was allowed to equilibrate for an additional 10 min. Curtain fractions were again collected for 10 min or more, depending on curtain flow rate. After equilibration to room temperature, the pH and conductivity of all collected fractions were measured, using a Radiometer PHM 64 pH meter equipped with a Radiometer GK 2321C combination electrode, and a YSI Model 31 Conductivity Bridge, calibrated with KCl standards.

IV. RESULTS

Over a wide range of field strengths, curtain flow rates, electrode buffer flow rates, and time, the pH/conductivity profiles of the fractionated buffer curtain showed the general form illustrated in Figure 3, which comprises a selection of experimentally obtained pH/conductivity profiles measured under a variety of conditions. All curves obtained using the Beckman CBE fitted with cellulose acetate membranes showed the following characteristic features:

- a) A small drop in pH and conductivity in fractions 1 and 2, with a gradual increase in pH and conductivity over the next 10 through 12 fractions (Region A in Fig. 3).
- b) Constant pH and conductivity values in the next 30 fractions (Region B in Fig. 3).
- c) A further increase in pH and conductivity in the last 3 through 4 fractions (Region C in Fig. 3).

Region C, while showing a clear trend towards higher pH's and conductivities, was not sufficiently well resolved by the fractionation procedure to allow analysis of gradient formation as a function of variations in the experimental conditions. The present results are, therefore, analyzed and discussed with reference to changes in pH and conductivity near the cathode membrane only (Region A, fractions 1 through 14) where good resolution of the fractionated curtain was obtained.

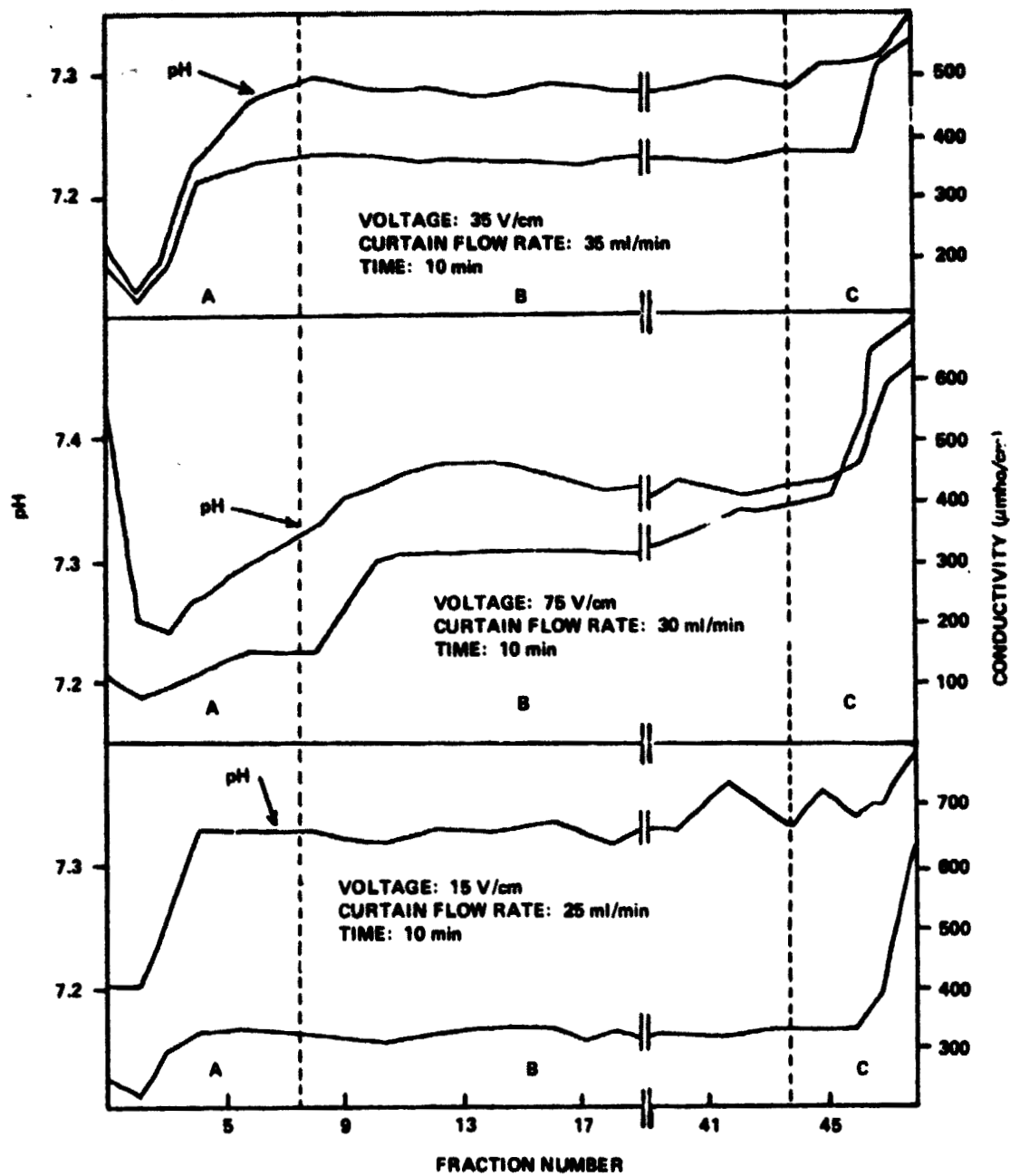


Figure 3. pH and conductivity profiles of R-1 buffer collected from the Beckman CPE under a variety of conditions. (For regions A, B, and C, see Section IV.)

The initial small decrease in pH and conductivity evident in fractions 1 and 2 of all the curves shown in Figure 3 was considered an artifact caused by the Poiseuille flow velocity distribution of curtain buffer adjacent to the cathode membrane. Thus, fractions 1 and 2 were contaminated with slow-moving buffer originating near the bottom of the electrophoresis chamber, and since this was not exposed to the electric field, these fractions showed pH/conductivity values closer to the standard values of the R-1 buffer. Similar considerations apply to other fractions sampled in these experiments, since parabolic flow velocity distributions occur also at the front and back walls of the electrophoresis chamber. Although the effect is less prominent some distance from the membranes, some uncertainty remains in the measured pH/conductivity values.

Figures 4 through 7 show the effect of four variables on the formation of pH/conductivity gradients near the cathode. The gradients were quantified in two ways: (a) total change of pH in Region A (ΔpH_A) and (b) distance of migration (in millimeters) of the pH discontinuity, defined as the boundary between Regions A and B. Figures 4 and 5, showing the influence of time and electrode buffer flow rate respectively, indicate that, within the ranges explored, these parameters had a minimal effect on pH gradient formation. The influence of curtain flow rate was more pronounced (Fig. 6), showing an inversely proportional relationship between curtain flow rate and pH gradient formation. This result was not unexpected since increased curtain flow rates tend progressively to swamp out the pH changes occurring near the electrode membranes. More interesting was the effect of electric field strength (Fig. 7) which was almost directly proportional to ΔpH_A and migration distance of the pH discontinuity, up to 50V/cm.

Figure 8 shows the pH profile measured in an experiment where electrophoresis buffer (R-1) replaced the 10X concentrated buffer generally circulating through the electrodes. Plateau values of pH were not attained until fraction 14, equivalent to 14-mm distance from the cathode membrane. In contrast, experiments carried out with concentrated R-1 buffer in the electrode compartments under similar conditions of electric field strength and curtain flow rate showed that plateau pH was established by fraction 8, only 8-mm distant from the membrane.

Figure 9 illustrates the pH/conductivity profile of curtain buffer in a continuous-flow electrophoresis experiment using the Hannig FF-5. The presence of an anion exchange membrane at the cathode reversed the slope of the pH gradient on the curtain side of the membrane.

ORIGINAL PAGE IS
OF POOR QUALITY

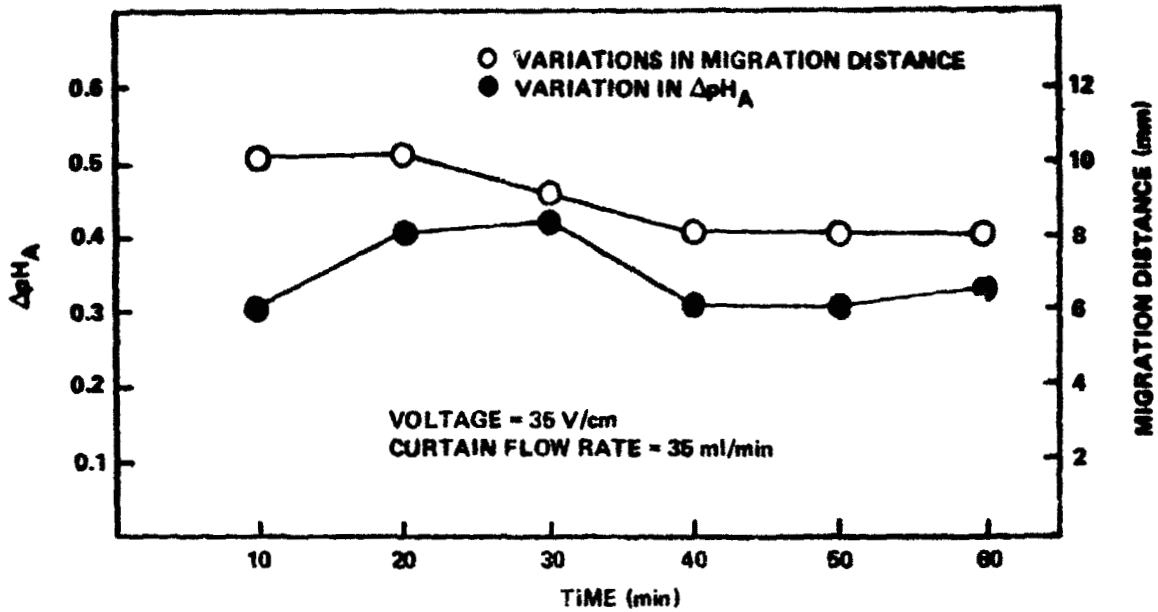


Figure 4. Effect of time on the change in pH in Region A and on the migration distance of the pH discontinuity.

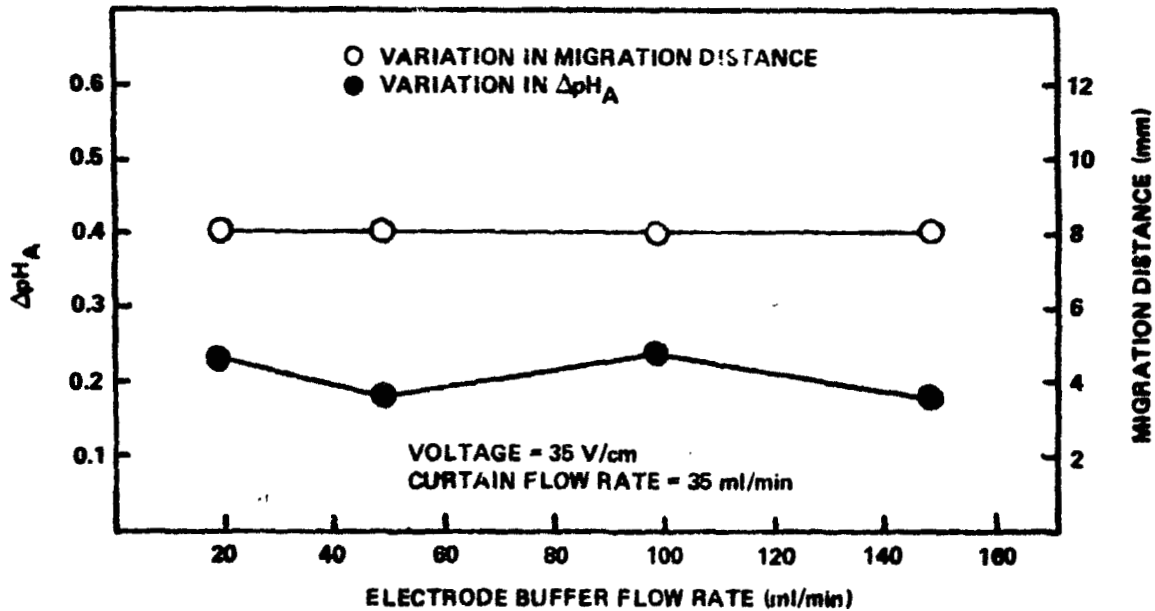


Figure 5. Effect of electrode buffer flow rate on the change in pH in Region A and on the migration distance of the pH discontinuity.

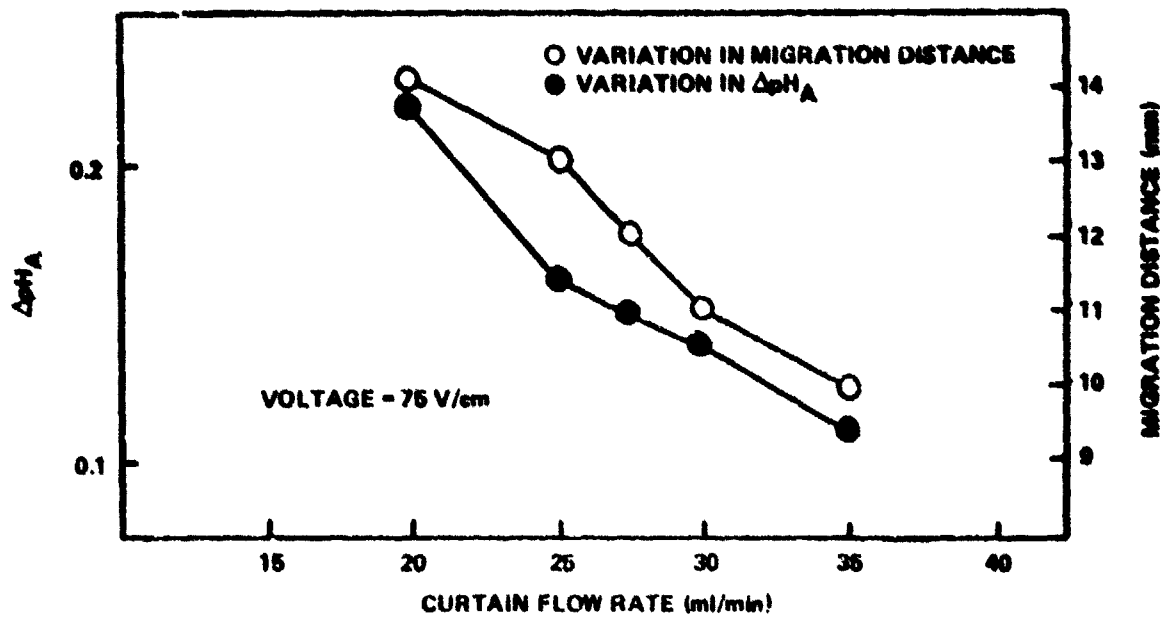


Figure 6. Effect of curtain flow rate on the change in pH in Region A and on the migration distance of the pH discontinuity.

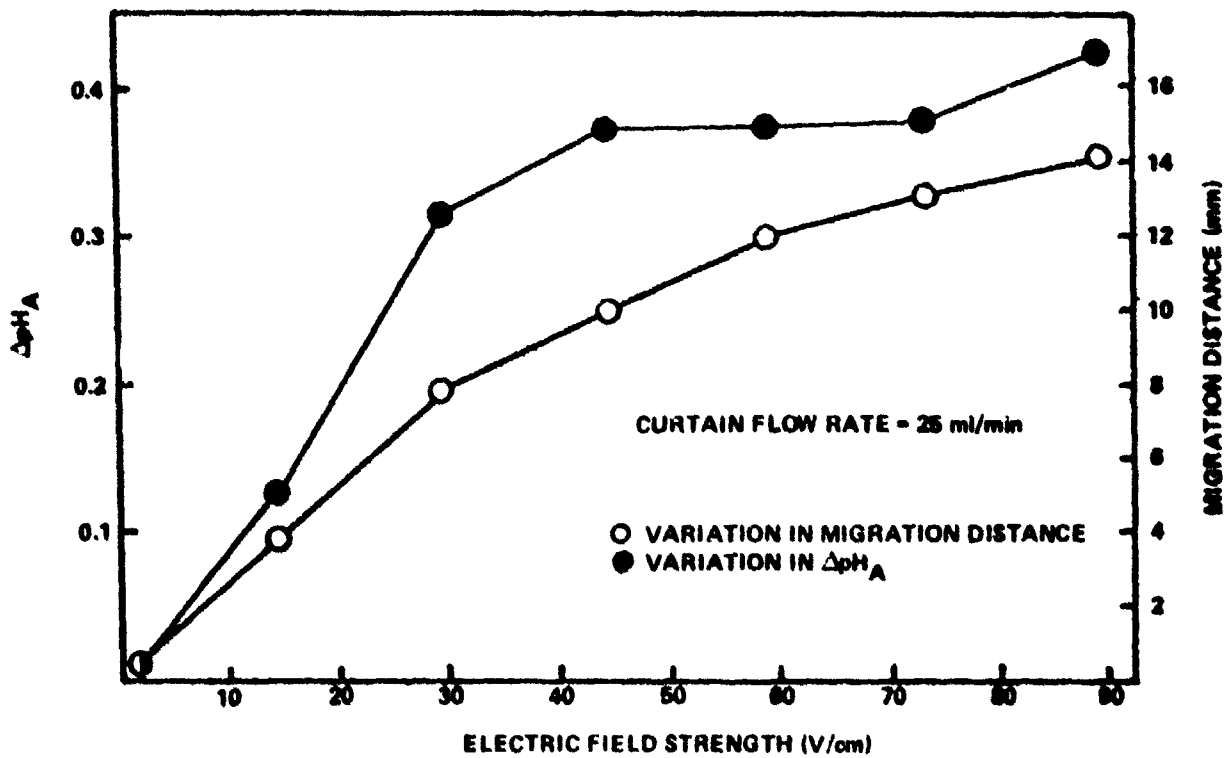


Figure 7. Effect of electric field strength on the change in pH in Region A and on the migration distance of the pH discontinuity.

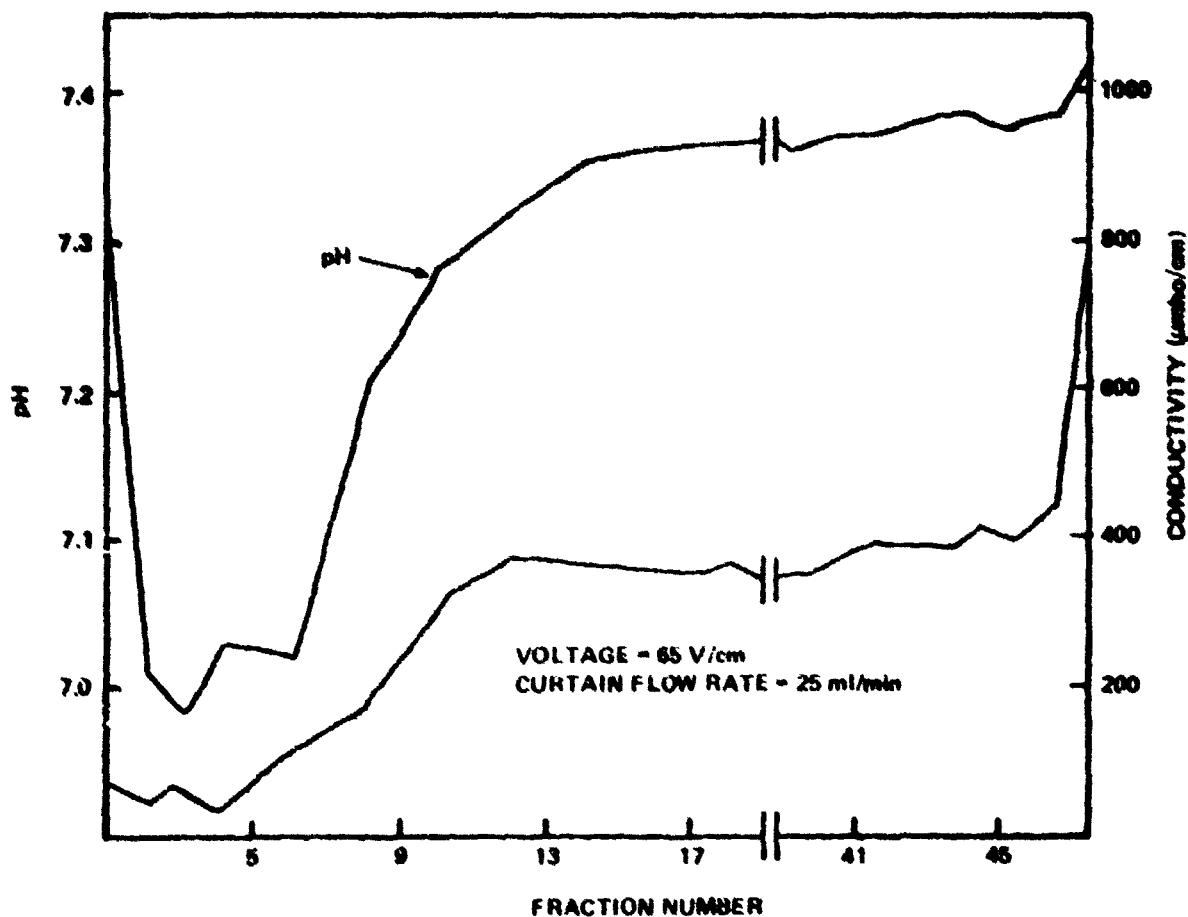


Figure 8. Conductivity and pH profile of R-1 buffer collected from Beckman CPE, with dilute R-1 buffer in both electrode compartments.

V. DISCUSSION

The final result indicated that the cellulose acetate membranes were causing the observed pH-conductivity changes in the Beckman CPE. At neutral pH, these membranes bear negative charges resulting from ionization of carboxyl groups throughout the membrane, the degree of polarization of the membrane being dependent on the electric field strength [14]. Thus, the dependence of the pH-conductivity gradients on field strength (Fig. 7) can be interpreted as resulting from membrane polarization.

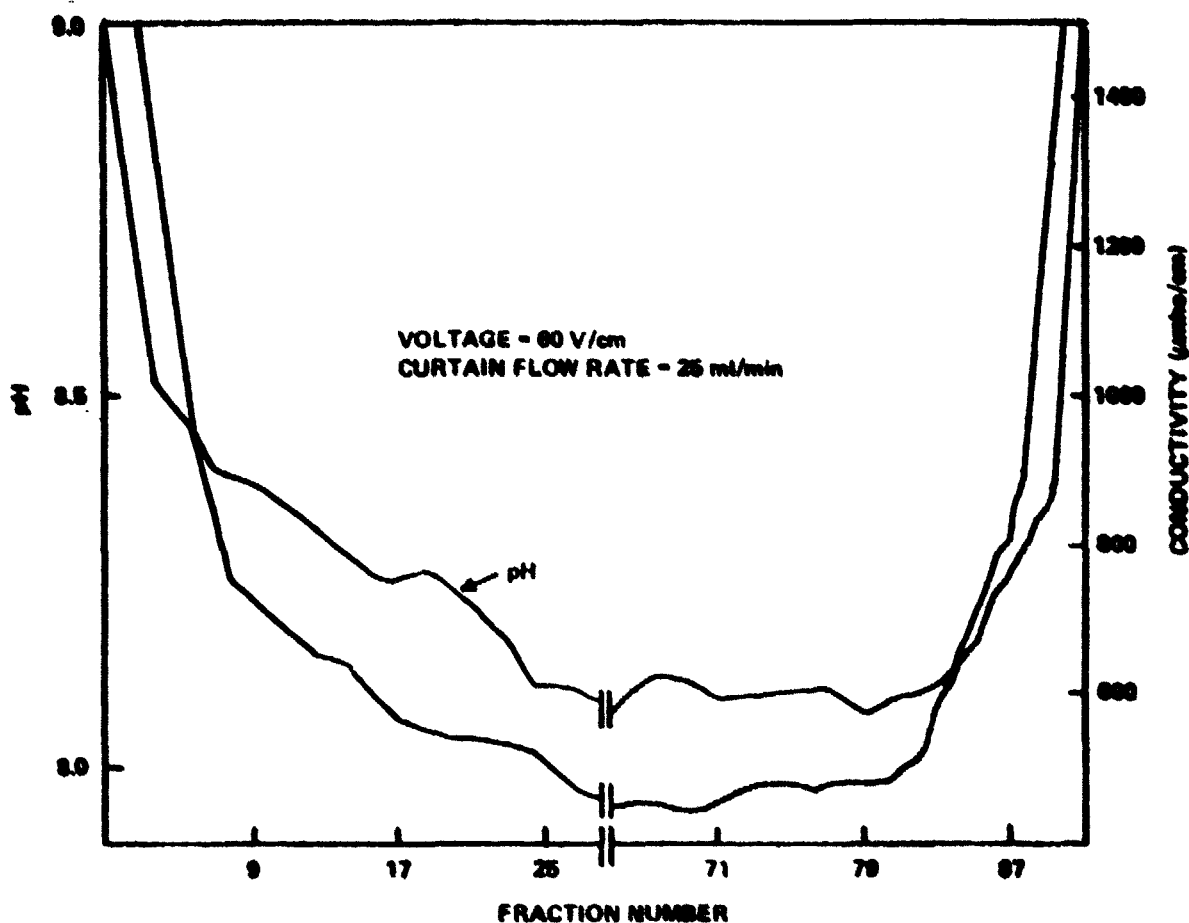


Figure 9. Conductivity and pH profile of R-1 buffer collected from Hannig FF-5 electrophoresis apparatus.

It is known that charged membranes reject ionic solutes by the phenomenon of Donnan ion exclusion. When a cation exchanger is placed in a dilute solution of a strong electrolyte, concentration differences occur between the two phases; cations predominate in the membrane, while free anions are concentrated in the solution. Since these ions are charged, simple diffusion tending to equalize the ionic concentrations would disturb the principle of electro-neutrality. Therefore, migration of cations into the solution and of anions into the membrane results in the accumulation of positive charges in the solution and of negative charges in the membrane. Thus, a potential difference, the Donnan potential, is established between the two phases. For a membrane containing fixed negative groups, the effect of Donnan potential is to exclude anions from the membrane. Since the

force exerted on an ion in an electric field is proportional to the ionic charge, the Donnan potential needed to balance counter-ion diffusion into the solution decreases with increasing counter-ion valency. Conversely, the efficiency of co-ion exclusion at a given Donnan potential is directly proportional to co-ion valency. Bhattacharyya et al. [15] have explained the rejection behavior of certain simple ions using Donnan theory. More recently, Lonsdale et al. [16] have published a model of ion rejection which extends Donnan's original equilibrium treatment to the nonequilibrium situation occurring in hyperfiltration. Indeed, this model has been applied to the separation of heavy metal salts by charged membrane ultrafiltration [17]. In this method, solute rejection increases with a decrease in the solute concentration on the high pressure side of the membrane.

Thus, the data presented in Figure 8, the effect of dilute electrode buffer, were interpreted as confirming solute rejection by the membrane. Reducing the electrode buffer concentration led to the formation of more pronounced cathodic pH gradients, in terms of lower pH and greater migration distance of the discontinuity into the buffer curtain.

Since the pH of the following buffer curtain is dependent on the Henderson-Hasselbalch equation,

$$\text{pH} = \text{pK}_1 + \log_{10} \frac{[\text{HPO}_4^{--}]}{[\text{H}_2\text{PO}_4^-]}$$

the reported changes in pH could only have resulted from adjustments of the relative concentrations of proton acceptors and donors in the buffer solution, i. e., divalent phosphate ions and monovalent phosphate ions. In the presence of an electric field, the mobility difference between these two ions could not of itself modify their relative concentrations in the electrophoresis buffer.

These considerations suggested a possible mechanism for the formation of the observed pH and conductivity gradients. In continuous-flow electrophoresis, negatively charged cathode membrane inhibits the passage of buffer anions by the Donnan exclusion mechanism. The divalent phosphate ions are more highly retarded than the monovalent ions since they possess approximately twice the charge of the latter. Therefore, on the curtain side of the cathode membrane, there occurs a relative decrease in divalent ion concentration, disturbing the Henderson-Hasselbalch ratio of buffer ions in the direction of decreased pH. In addition, the fall in divalent ion concentration in this region is reflected in a

decrease in the measured conductivity, which is a function of the total number of current-carrying ion species present. At a negatively charged anode membrane, a similar selective retention of buffer ions occurs, this time resulting in a relative increase in divalent ion concentration on the curtain side of the membrane, leading to increased pH and conductivity measurements in this region.

The condition of this mechanism that buffer pH and conductivity should be lowered near the cathode, and elevated near the anode, was fulfilled by the data shown in Figure 3. The effects of replacing the negatively charged cathode membrane with an anion exchange membrane (Fig. 9) further support the mechanism, since in this case the Donnan potential has reversed polarity. Anion exchange membranes are characterized by the presence of basic groups (e.g., $-NR_2$ or $=NR$) which at neutral pH are positively charged, thereby favoring passage of divalent buffer ions over monovalent ions. Consequently, curtain buffer pH was increased, rather than decreased, in the presence of an anion exchange membranes at the cathode.

The deviations in buffer pH and conductivity discussed in this report have several consequences for the separation of charged species by continuous-flow electrophoresis. Zone electrophoresis, in contrast to isoelectric focusing and isotachopheresis, calls for constant buffer pH and conductivity in the separation medium. This requirement ensures that the electrophoretic mobility of the separands is invariant during the separation. Samples to be separated by continuous-flow electrophoresis generally occupy only the central portion of the buffer curtain, where pH and conductivity are constant; however, with samples which display a wide range of differing electrophoretic mobilities, the need to confine the sample streak to the center of the buffer curtain dictates the use of low field strengths, and subsequent loss of resolution. For this reason alone, the development of nonpolarizable membranes could be significant for continuous-flow electrophoresis.

Another consequence of buffer instability near the membranes is the generation of lateral temperature gradients at the edges of the buffer curtain. The fall in buffer conductivity to approximately $100 \mu\text{mho/cm}$ near the cathode increases the resistance in this region and, consequently, the temperature of the buffer. Under these conditions, the temperature difference between the mid-portion of the chamber and the cathode membrane is approximately 10°C . This temperature gradient is analogous to the longitudinal gradients encountered in capillary isotachopheresis, where higher temperatures prevail in the terminating buffer adjacent to the cathode than are attained in the leading buffer adjacent to the anode. In continuous-flow electrophoresis, however, the temperature

gradient is normal to the gravitational vector, and convective disturbances are likely to arise at the edges of the buffer curtain, especially at the low curtain buffer flow rates necessary for optimal resolution. It is possible that the slow drift of sample streaks characteristic of continuous-flow electrophoresis owes its existence at least partly to the membrane-associated thermal convection. Certainly the phenomenon should be considered in all theoretical modeling of the fluid dynamics of continuous-flow electrophoresis.

Lastly, the stability of the membrane-generated pH gradients with time suggests a possible application in continuous-flow isoelectric focusing. The high cost of Ampholines (LKB, Bromma Sweden), hitherto widely used to establish pH gradients, and their unpredictable conductivity courses have recently encouraged investigators [18,19] to re-examine the possibilities of pH gradient formation using simple buffers. The present study indicated that stable shallow pH gradients can be formed in the region of charged semi-permeable membranes. The presence of a linear conductivity gradient in such gradients, while running counter to the accepted requirements for isoelectric focusing, may conceivably add another separative parameter to the technique, although further experiments are needed to clarify this point.

REFERENCES

1. Svensson, H. and Brattsten, I.: An Apparatus for Continuous Electrophoretic Separation in Flowing Liquids. *Arkiv. Kemi.*, vol. 1, 1949, p. 401.
2. Barrolier, V. J., Watzke, E., and Gibian, H.: Einfache Apparatur für die Tragerfreie Präparative Durchlauf-Elektrophorese. *Z. Naturforsch.*, vol. 13b, 1958, p. 754.
3. Hannig, K.: Die Tragerfreie Kontinuierliche Ablenkungselektrophorese und ihre Anwendung. *Z. Anal. Chem.*, vol. 181, 1961, p. 244.
4. Strickler, A. and Sacks, T.: Focusing in Continuous Flow Electrophoresis Systems by Electrical Control of Effective Cell Wall Zeta Potentials. *Ann. N. Y. Acad. Sci.*, vol. 209, 1973, p. 497.
5. Rhodes, P. H.: High-resolution, Continuous Flow Electrophoresis in Microgravity. NASA TM-78158, 1978.
6. Semon, H. W.: Investigation of Flow Stability in the SPAR Wide-gap Electrophoretic Separation Chamber. NASA Contract NAS8-31036, G. E. Company, Philadelphia, Pennsylvania, 1977.
7. Ostrach, S.: The Influence of Convection in Continuous Flow Electrophoresis. ESA Special Publication, No. 114, 1976.
8. Hannig, K.: Electrophoretic Separation of Cells and Particles by Continuous Free-flow Electrophoresis. *Techniques of Biochemical and Biophysical Morphology*, D. Glick and R. Rosenbaum (editors), vol. 1, John Wiley and Sons, Inc., 1972, pp. 191-231.
9. Seaman, G. V. F.: Electrophoretic Separator Experiments. NASA Contract NAS8-32609, University of Oregon Health Sciences Center, Portland, Oregon, 1978.
10. Snyder, R. S.: Continuous Flow Electrophoretic Separator Development for SPAR. Proposal to NASA, 1978.
11. Brattsten, I.: Continuous Zone Electrophoresis by Crossed Velocity Fields in a Supporting Medium. *Arkiv. Kemi.*, Band 8, No. 23, 1954, p. 23.

REFERENCES (Concluded)

12. Zeller, K., Loser, R., Pascher, G., and Hannig, K.: Free-Flow Electrophoresis 11: Analysis of the Method with Respect to Preparative Cell Separation. *Hoppe-Seyler's Z. Physiol. Chem.*, vol. 356, 1975, p. 1225.
13. Strickler, A.: Preparative Electrophoresis Experiment Design for Space. Final Report, NASA Contract NAS8-28474, Beckman Instruments, Inc., Anaheim, California, 1974.
14. Bender, M., Khazai, B., and Dougherty, T. E.: Diffusion and Sorption of Simple Ions in Cellulose Acetate - Semipermeability. *J. Colloid Interface Sci.*, vol. 63, No. 2, 1976, p. 346.
15. Bhattacharyya, D., McCarthy, J. J., and Grieves, R. B.: Charged Membrane Ultrafiltration of Inorganic Ions in Single and Multi-salt Systems. *AIChE Journal*, vol. 20, 1974, p. 1206.
16. Lonsdale, H. K., Walch, A., and Pusch, W. J.: Donnan-membrane Effects in Hyperfiltration of Ternary Systems. *J. Chem. Soc., Faraday Trans.*, vol. 71, 1975, p. 501.
17. Bhattacharyya, D., Moffitt, M., and Grieves, R. B.: Charged Membrane Ultrafiltration of Toxic Metal Oxyanions and Cations from Single and Multi-salt Aqueous Solutions. *Sep. Sci. and Technol.*, vol. 13, No. 5, 1978, p. 449.
18. Rilbe, H.: Steady-state Rheoelectrolysis. *J. Chromatog.*, vol. 159, 1978, pp. 193-205.
19. Boltz, R. C., Miller, T. Y., Todd, P., and Kukulinsky, N. E.: A Citrate Buffer System for Isoelectric Focusing and Electrophoresis of Living Mammalian Cells. NASA Preprint Series No. 78-122, 1978.

APPROVAL

CONTINUOUS-FLOW ELECTROPHORESIS: MEMBRANE-ASSOCIATED DEVIATIONS OF BUFFER pH AND CONDUCTIVITY

By Adam J. K. Smolka and Janice K. McGuire

The information in this report has been reviewed for technical content. Review of any information concerning Department of Defense or nuclear energy activities or programs has been made by the MSFC Security Classification Officer. This report, in its entirety, has been determined to be unclassified.



ROBERT S. SNYDER
Chief, Separation Processes Branch



ROBERT J. NAUMANN
Chief, Space Processing Division



CHARLES A. LUNDQUIST
Director, Space Sciences Laboratory